Optimal and Suboptimal Velocity-Aiding for VOR/DME Systems

NORBERT B. HEMESATH*
Collins Radio Company, Cedar Rapids, Iowa

The use of onboard velocity sensors to improve the positional accuracy of VOR/DME navigation systems is described. The analytical formulation of the problem combines velocity and VOR/DME data in an optimal filter. Suboptimal filters of reduced complexity are also described. Performance analyses are given for the specific cases where either an inertial system or an air data system is the available velocity sensor, and comparisons are made between the rms performance of optimal and suboptimal filters. The analyses show that velocity-aiding can substantially improve positional accuracy and that suboptimal filtering can be achieved without disastrous performance penalties.

Introduction and Problem Statement

THE VOR/DME† system has been the backbone of domestic air navigation for some 15 or 20 years. Although the system has provided yeoman service over that period, it is well known that its navigational data contain significant errors produced by multipath propagations which contaminate the information-bearing radio signals.

The DME determines range by measuring the round-trip propagation time between the aircraft and the ground station. It transmits pulses, and therefore, with careful receiver design is essentially immune from the effects of multipath propagation. The VOR, on the other hand, determines bearing-to-station by observing the phase relationship between a spatial radiation pattern and a reference signal. Any radiated energy which is reflected perturbs the desired spatial pattern, thereby altering the desired phase relationship and producing an error in indicated bearing at the receiver output. In the vicinity of a station any man-made structure, such as a large building, or any topographic anomaly, such as a mountain, acts as a reflector of radiated energy and is therefore potentially a source of VOR error. A somewhat detailed discussion of this problem is given in Refs. 1 and 2.

To an aircraft in flight the reflection-induced distortion of the spatial radiation pattern appears at the output of a VOR receiver as a slowly-changing quantity. This error may be as large as several degrees and its frequency is typically 0.5 to 3 or 4 cycles/min. When the VOR is used for guidance, the error in its output produces both aircraft positioning error and a considerable amount of extraneous bank activity as the aircraft attempts to follow the errors. Both effects are objectionable; the first because it represents a departure from assigned course, and the second because it causes passenger and crew discomfort.

Because of the undesirable dynamic effects of coupling the VOR error into the flight control system, much effort has been expended in devising methods to reduce that error. Moreover, the need in recent years for more precise approach guidance to both instrumented and uninstrumented runways in crowded terminal areas has produced the demand for navigational accuracies which are beginning to tax the capabilities of the present system. Consequently, great interest has been expressed in upgrading the precision of navigational data derived from VOR/DME. As a solution to this problem a new, more accurate system could be developed and deployed, but the economic realities of this revolutionary approach preclude its adoption in the near future. A more realistic short-term approach is to use onboard signal processing techniques to combine VOR/DME data with information from other readily available sensors.

Since most transport aircraft carry some type of velocity sensor this paper considers the question of finding the best way to use an onboard velocity source to augment VOR/DME data, and finding what tradeoffs can be made between mechanization complexity and performance. The paper is organized into the following major segments: 1) general formulation, 2) error descriptions, 3) optimal mechanization, 4) suboptimal mechanizations, and 5) performance comparisons.

Data Utilization Philosophy

Clearly an onboard velocity source and the VOR/DME system sense related kinematic information. If the individual measurements contained no errors and if they were referred to the same coordinate system a properly initialized integration of the velocity components would precisely equal the VOR/DME-derived position. It is this redundant information which we will employ to reduce the effect of VOR errors.

In general the two measurements can be combined in some "best" way—namely with an optimum filter—and our goal is to show how this is done. However, in order to develop the optimal mechanization we must have a description of the errors in our two data sources.

Error Descriptions

The design of an optimum filter requires a complete dynamic model of the process to be filtered. Consequently, this section of the paper is devoted to development of appropriate models for VOR/DME errors and for errors in the velocity source.

VOR/DME Errors

The geometry of VOR/DME position determination in the plane is depicted in Fig. 1 where the ground station is at the origin of the coordinate system (x-east, y-north). The aircraft, located at (x, y) has a bearing α and a range R with respect to the station so its coordinates are

$$\begin{aligned} x &= R\sin\alpha \\ y &= R\cos\alpha \end{aligned} \tag{1}$$

The VOR measures α with an error $\Delta\alpha$, and the DME measures R with an error ΔR, so the coordinates determined by these measurements are

$$\begin{aligned} y_m &= x+\Delta x = (R+\Delta R)\sin(\alpha+\Delta\alpha) \\ y_m &= y+\Delta y = (R+\Delta R)\cos(\alpha+\Delta\alpha) \end{aligned} \tag{2}$$

Presented as Paper 70-1024 at the AIAA Guidance, Control and Flight Mechanics Conference, Santa Barbara, Calif., August 17–19, 1970; submitted November 13, 1970; revision received September 2, 1971.

* Technical Staff, Avionics System Division.

† VOR (very high frequency omnirange); DME (distance measuring equipment). The VOR and the DME measure bearing and distance, respectively, with respect to a ground station of known location.

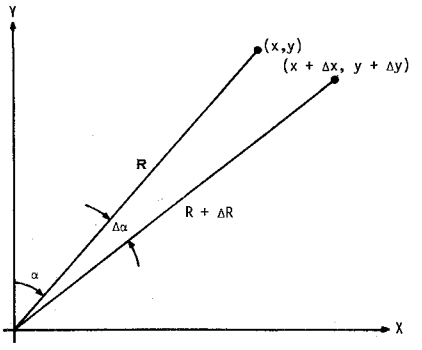

Fig. 1 VOR/DME position fixing.

For small $\Delta\alpha$ and ΔR the errors, Δx and Δy, in the measured coordinates are to first order approximation

$$\begin{bmatrix}\Delta x\\ \Delta y\end{bmatrix}=\begin{bmatrix}R\cos\alpha\sin\alpha\\ -R\sin\alpha\cos\alpha\end{bmatrix}\begin{bmatrix}\Delta\alpha\\ \Delta R\end{bmatrix} \tag{3}$$

The sensor errors, $\Delta\alpha$ and ΔR, are treated as independent, zero-mean, stochastic processes with rms values $\sigma_{\Delta\alpha}$ and $\alpha_{\Delta R}$, respectively. Moreover, each is assumed to be exponentially auto-correlated, so we have

$$E[\Delta\alpha(t)\Delta\alpha(t+\tau)]=\sigma_{\Delta\alpha}^2\exp(-\beta_{\Delta\alpha}|\tau|) \tag{4}$$

$$E[\Delta R(t)\Delta R(t+\tau)]=\sigma_{\Delta R}^2\exp(-\beta_{\Delta R}|\tau|) \tag{5}$$

Experience with the VOR and DME sensors indicates that the exponential and stationarity assumptions are reasonable and valid to use in modeling their errors. Examination of a substantial number of FAA data records has produced the numerical values in Table 1 for the parameters of the correlation functions. The correlation times are, in general, velocity dependent. The VOR error has a fixed spatial pattern, and it is the motion of the aircraft through this pattern that produces the time variation of the error. To the navigation processor the time variation of DME error will depend upon how long each station is used and hence upon the aircraft velocity. The numerical values given for the correlation times are for high subsonic speeds.

Table 1 VOR/DME error parameters

Parameter	VOR	DME
rms value	$\sigma_{\Delta\alpha}=1.15°$	$\sigma_{\Delta R}=0.2$ naut mile
Correlation time	$1/\beta_{\Delta\alpha}=10$ sec	$1/\beta_{\Delta R}=300$ sec

To assess the positional accuracy of the VOR/DME system the sensor errors, $\Delta\alpha$ and ΔR, must be related to some measure of position error. A convenient measure of system performance is the rms radial‡ error defined as

$$\sigma_R=[E(\Delta x^2+\Delta y^2)]^{1/2}$$

where $E(\cdot)$ denotes mathematical expectation. Utilizing Eq. (3) in this definition we find

$$\sigma_R=[R^2\sigma_{\Delta\alpha}^2+\sigma_{\Delta R}^2]^{1/2} \tag{6}$$

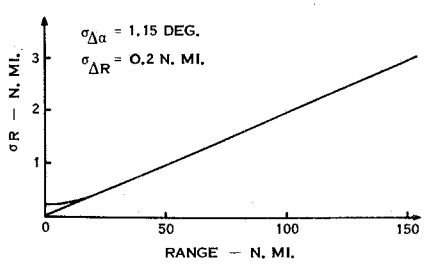

Fig. 2 VOR/DME radial position error.

‡Radial as used here refers to the radius of a circle within which the navigation system errors are expected to lie, and it should not be confused with the term "VOR radial."

Figure 2 is a plot of this radial error function for the rms values of VOR and DME error given in Table 1. The straight line through the origin is the VOR contribution to radial error, so it is quite apparent that beyond 15 or 20 miles from the station the DME contribution is insignificant. Thus the radial error curve for uncomplemented VOR/DME is essentially a linear function of range from the station, and its slope is the rms VOR error. Later we shall compare this curve to a similar one for complemented systems.

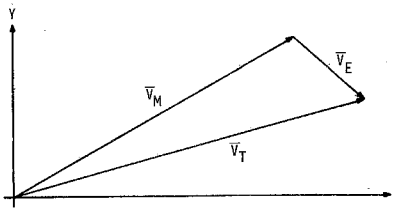

Fig. 3 Velocity vector relationships.

Velocity Source Errors

Figure 3 shows the simple vector relationships which must hold for any on-board velocity measurement. The true velocity vector $\bar{V}_T$ is equal to the measured velocity vector $\bar{V}_M$ plus an error vector $\bar{V}_E$, i.e.,

$$\bar{V}_T=\bar{V}_M+\bar{V}_E \tag{7}$$

The following two scalar equations can be written in place of the vector relation

$$\begin{aligned}V_{Tx}&=V_{Mx}+V_{Ex}\\ V_{Ty}&=V_{My}+V_{Ey}\end{aligned} \tag{8}$$

The integrals of the components V_{Mx} V_{My} provide measurements x_M and y_M of the true aircraft position components, x and y

$$\begin{aligned}\int_0^t V_{Mx}\,d\tau&=x_M(t)=x(t)+\Delta x(t)\\ \int_0^t V_{My}\,d\tau&=y_M(t)=y(t)+\Delta y(t)\end{aligned} \tag{9}$$

Utilizing the expressions in Eqs. (8) we observe that the error components are

$$\begin{aligned}\Delta x(t)&=-\int_0^t V_{Ex}(\tau)\,d\tau\\ \Delta y(t)&=-\int_0^t V_{Ey}(\tau)\,d\tau\end{aligned} \tag{10}$$

Thus position components derived by integrating velocity contain errors which are simply the integrals of the corresponding velocity error components. Because the velocity errors are stochastic, the rms radial position error grows in proportion to the integration time.

Data from any velocity source can be treated in the manner described above even though the nature of the error vector $\bar{V}_E$ will be quite different from one source to another. Error models for two commonly encountered sources are given next.

Air Data Errors

An airspeed sensor and a heading reference comprise an Air Data System which is designed to measure the true airspeed vector $\bar{V}_A$. Figure 4 is a vector diagram of the various quantities involved in the measurements. The true velocity vector $\bar{V}_T$ is equal to the true airspeed vector $\bar{V}_A$ plus the wind vector $\bar{V}_W$. However, the Air Data System measures $\bar{V}_A$ plus a vector $\bar{V}_s$ attributable to sensor errors, i.e.,

$$\bar{V}_M=\bar{V}_A+\bar{V}_s \tag{11}$$

Substituting for $\mathbf{V}_A$, Eq. (11) becomes

$$\bar{V}_M=\bar{V}_T-\bar{V}_W+\bar{V}_s \tag{12}$$

If the vector sum of $\mathbf{V}_W$ and $\mathbf{V}_s$ is redefined as

$$\bar{V}_E=\mathbf{V}_W-\bar{V}_s \tag{13}$$

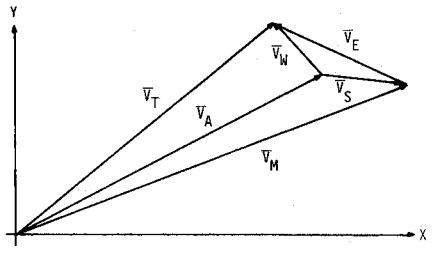

Fig. 4 Air Data System vector relationships.

then $\mathbf{V}_E$ is the system's total velocity error vector as in Eq. (7). Equation (13) says that, to an observer, the effects of airspeed and heading reference errors are indistinguishable from wind.

Consequently, to describe Air Data System velocity error, one must characterize $\mathbf{V}_E$. The largest component of this vector is wind, since the error in a good quality airspeed sensor is only a few knots and a precision heading sensor will typically produce less than 10 knots error at high subsonic speeds. Thus we shall model the components of $\mathbf{V}_E$ as if they consisted of wind only, but bear in mind that they also contain contributions from heading and airspeed errors. The components are assumed to be uncorrelated, stationary, stochastic processes each with exponential autocorrelation. High-frequency winds which buffet the aircraft displace it negligibly, so we need only characterize the slowly-changing, large magnitude winds. Because data to describe this wind condition are very sparse, the choice of the rms value and the correlation time of the components is admittedly somewhat arbitrary. Nevertheless, the numerical values given below appear realistic.

$$(1/\beta) = 10\,\text{min}, \qquad \sigma = 40\,\text{knots}$$

The correlation time as viewed from an aircraft is velocity dependent, and the value cited is for high subsonic speeds.

Inertial Velocity Errors

An inertial navigation system provides a very precise measurement of velocity, and the dynamics of its error propagation have been well developed and are well understood (Ref. 3). Consequently, it would seem that standard inertial error models could be employed without further discussion. Although this is possible the standard model is of rather high dimension and therefore cumbersome to use in an optimal mechanization. If one is principally interested in the inertial velocity outputs and not particularly concerned about correcting the instrument errors of the inertial system, a simple low-pass model of inertial velocity errors is quite adequate. The velocity error of an undamped inertial system is nonstationary since its rms value grows slowly with time. The error spectrum is clearly low-pass in nature with a break frequency at the 84 min Schuler period. For an inertial system in the 1–2 naut mph class operating up to 6 or 8 hr at a time a reasonable upper bound on rms velocity error is about 4 knots. This 4 knot value will be used for rms, and the error will be assumed exponentially-autocorrelated with 10 min correlation time. Each of these assumptions is a bit harsh, but the conservative error model is used to compensate for the fact that we are using a stationary model for a process which is, in fact, nonstationary.

Optimal Mechanization

We developed error models for both the VOR/DME system and the velocity source in the preceding section. In this section we shall see how data from these two sources is optimally combined and what role the error models play.

Let $\bar{\mathbf{P}}_1$ and $\bar{\mathbf{P}}_2$ be the position vectors simultaneously obtained from VOR/DME and from integrated velocity at any arbitrary time. Each measurement will consist of the true but unknown position $\bar{\mathbf{P}}$ plus an error term, i.e.,

$$\bar{\mathbf{P}}_1 = \bar{\mathbf{P}} + \Delta\bar{\mathbf{P}}_1, \qquad \bar{\mathbf{P}}_2 = \bar{\mathbf{P}} + \Delta\bar{\mathbf{P}}_2$$

where $\Delta\bar{\mathbf{P}}_1$ and $\Delta\bar{\mathbf{P}}_2$ are the error vectors in VOR/DME and integrated velocity measurements, respectively. The difference between these two measured positions is a function of the error vectors only. This fact is of fundamental significance for it says that the effects of sensor errors can be isolated from the kinematic data which the system is designed to measure, and it suggests the possibility of processing the position differences in order to estimate the sensor errors. The estimated errors could then be applied as corrections to the sensed data. We accomplish the estimation process, which can be carried out to the extent that sensor errors have individual characteristics which permit them to be separated from one another, through application of optimum (Kalman) filter methods.

The position difference vector can be related to sensor errors by using Eqs. (3) and (10)

$$[\Delta\bar{\mathbf{P}}_1 - \Delta\bar{\mathbf{P}}_2] = \begin{bmatrix} y_1 \\ y_2 \end{bmatrix} = \begin{bmatrix} R\cos\alpha\sin\alpha - 1 & 0 \\ -R\sin\alpha\cos\alpha & 0 & -1 \end{bmatrix} \begin{bmatrix} \Delta\alpha \\ \Delta R \\ x_E \\ y_E \end{bmatrix} \tag{14}$$

where

$$x_E(t) = -\int_0^t V_{Ex}(\tau)\,d\tau$$

$$y_E(t) = -\int_0^t V_{Ey}(\tau)\,d\tau$$

Clearly y_1 and y_2 are the differences between the measured position components in the X and Y directions, respectively, and they are linearly dependent upon the quantities in the state vector on the right side of Eq. (14). Now, given a dynamic model describing the evolution of the state vector, there exists a linear filter which, operating on the measurables y_1 and y_2, provides minimum mean square error estimates of the state variables.[4]

The information needed to complete the state equation is implicit in the spectral representation of the errors. In particular a process with an exponential autocorrelation function satisfies a differential equation of the form[5]

$$\dot{p} = -\beta p + w(t) \tag{15}$$

where $E[p_0^2] = \sigma^2$ and $w(t)$ is white noise of spectral magnitude $2\beta\sigma^2$. Since exponential models were used for all the error sources discussed earlier, the following state equation is readily deduced by writing in vector-matrix form the various scalar equations of the form Eq. (15) which describe the individual error parameters

$$\frac{d}{dt}\begin{bmatrix} x_E \\ y_E \\ V_{Ex} \\ V_{Ey} \\ \Delta\alpha \\ \Delta R \end{bmatrix} = \begin{bmatrix} 0 & 0 & 1 & 0 & 0 & 0 \\ 0 & 0 & 0 & 1 & 0 & 0 \\ 0 & 0 & -\beta_x & 0 & 0 & 0 \\ 0 & 0 & 0 & -\beta_y & 0 & 0 \\ 0 & 0 & 0 & 0 & -\beta_{\Delta\alpha} & 0 \\ 0 & 0 & 0 & 0 & 0 & -\beta_{\Delta R} \end{bmatrix} \begin{bmatrix} x_E \\ y_E \\ V_{Ex} \\ V_{Ey} \\ \Delta\alpha \\ \Delta R \end{bmatrix} + \begin{bmatrix} 0 \\ 0 \\ W_1 \\ W_2 \\ W_3 \\ W_4 \end{bmatrix} \tag{16}$$

All the parameters in this equation have been specified, and the covariance matrix of the white noise vector is fixed by the rms values of the error sources.

With the completion of the state equation all the information required by the optimum filter is avilable. The filter processes the two components of position difference which are obtained every ΔT seconds and generates estimates of the VOR error, DME error, and components of velocity error. Figure 5 shows how the estimates are applied as corrections to the measured data. The corrected data are then best estimates of the desired information.

Suboptimal Mechanizations

Although the optimal velocity-aided VOR/DME mechanization is extremely desirable from a system performance viewpoint, in a real-time, airborne application both its computation time requirements and its memory requirements quickly become burdensome. Consequently, there is strong motivation to consider suboptimal filter mechanizations which give up a small

increment in performance for a sizable reduction in computation and memory requirements.

Most of the optimal filter complexity lies in the computation of the time-varying gain matrix which determines how the most recently measured data is weighted with respect to all past data. This computation requires a significant amount of manipulation and multiplication of matrices whose dimension is that of the system dynamic model. This dimension is 6 in the velocity-aided VOR/DME problem as formulated. The gain matrix computation can be simplified in two basic ways: 1) a simplified algorithm can be used to generate the matrix, 2) a reduced dimension dynamic model can be used.

Using the first approach one could precompute the gain matrix and store it either functionally (least-squares fit, for example) or in a tabular form. However, the geometry with respect to the ground station varies so much that computer memory requirements for either the functional or the tabular representation are excessive if the gain matrix is to be retained with reasonable fidelity. Consequently we shall use the second approach to develop three specific suboptimal mechanizations for the velocity-aided VOR/DME problem.

Delection of DME Error Model

Elimination of the DME error from the system error model is a first approach to reducing the complexity of the optimal mechanization. This step is equivalent to assuming that the DME measures range to station perfectly. Although this assumption is not quite valid, the DME is an extremely accurate ranging device, and, as demonstrated previously, its contribution to radial error is insignificant relative to that of the VOR except at very short ranges. Thus the assumption is a reasonable one to use in a suboptimal design. The performance of this design is compared to the optimal later in this paper.

Decoupled Channel Mechanizations

The optimal filter processes two-dimensional information—the two components of the position difference term. The components could also be treated as two separate one-dimensional problems. Since the number of operations and the complexity of an optimal filter is roughly proportional to the third power of the system dimension, clearly two separate problems of dimension three are much easier to handle than one of dimension six. However, as will become clear, when correlation exists between the two position components, the decomposition of a two-dimensional problem into two single channel problems destroys some information. Nevertheless, because of the substantial reduction in complexity this approach offers, it is considered next.

Returning to the position difference expression (14) let us make a different choice of state variables by introducing the following two terms

$$\begin{aligned} \Delta x &= \Delta\alpha \cos\alpha \\ \Delta y &= -\Delta\alpha \sin\alpha \end{aligned} \tag{17}$$

Then if the DME error ΔR is omitted Eq. (14) can be rewritten as

$$[\Delta\bar{\mathbf{P}}_1 - \Delta\bar{\mathbf{P}}_2] = \begin{bmatrix} y_1 \\ y_2 \end{bmatrix} = \begin{bmatrix} R & -1 & 0 & 0 \\ 0 & 0 & R & -1 \end{bmatrix} \begin{bmatrix} \Delta x \\ x_E \\ \Delta y \\ y_E \end{bmatrix} \tag{18}$$

Assuming that Δx and Δy have the same correlation time as $\Delta\alpha$, the state model Eq. (16) can be replaced by the following one

$$\frac{d}{dt}\begin{bmatrix} x_E \\ V_{Ex} \\ \Delta x \\ y_E \\ V_{Ey} \\ \Delta y \end{bmatrix} = \left[\begin{array}{ccc:ccc} 0 & 1 & 0 & 0 & 0 & 0 \\ 0 & -\beta_x & 0 & 0 & 0 & 0 \\ 0 & 0 & -\beta_{\Delta\alpha} & 0 & 0 & 0 \\ \hdashline 0 & 0 & 0 & 0 & 1 & 0 \\ 0 & 0 & 0 & 0 & -\beta_y & 0 \\ 0 & 0 & 0 & 0 & 0 & -\beta_{\Delta\alpha} \end{array}\right] \begin{bmatrix} x_E \\ V_{Ex} \\ \Delta x \\ y_E \\ V_{Ey} \\ \Delta y \end{bmatrix} + \begin{bmatrix} 0 \\ W_1 \\ W_2 \\ 0 \\ W_3 \\ W_4 \end{bmatrix} \tag{19}$$

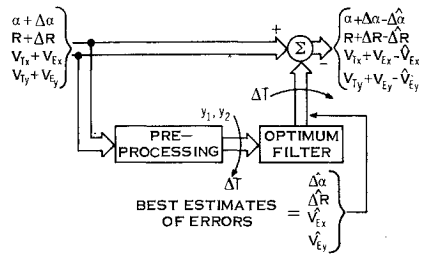

Fig. 5 System information flow.

However, the new variables Δx and Δy are correlated because each is a function of the VOR error. Specifically, using Eq. (17)

$$E[\Delta x\, \Delta y] = -\sin\alpha \cos\alpha \sigma_{\Delta\alpha}^2$$

This means that the white noise forcing functions W_2 and W_4 are correlated, and therefore the covariance matrix of the white noise vector on the right is no longer diagonal. This matrix is

$$Q = \left[\begin{array}{ccc:ccc} 0 & 0 & 0 & 0 & 0 & 0 \\ 0 & 2\beta_x\sigma_x^2 & 0 & 0 & 0 & 0 \\ 0 & 0 & q_{33} & 0 & 0 & q_{36} \\ \hdashline 0 & 0 & 0 & 0 & 0 & 0 \\ 0 & 0 & 0 & 0 & 2\beta_y\sigma_y^2 & 0 \\ 0 & 0 & q_{36} & 0 & 0 & q_{66} \end{array}\right] \tag{20}$$

where

$$\begin{aligned} q_{33} &= 2\beta_{\Delta\alpha}\cos^2\alpha\sigma_{\Delta\alpha}^2 \\ q_{66} &= 2\beta_{\Delta\alpha}\sin^2\alpha\sigma_{\Delta\alpha}^2 \\ q_{36} &= 2\beta_{\Delta\alpha}\sin\alpha\cos\alpha\sigma_{\Delta\alpha}^2 \end{aligned}$$

The optimal mechanization is dependent upon the state transition matrix Φ which is the solution to the homogeneous part of Eq. (19), the output matrix in Eq. (18), and the covariance matrix Q given in Eq. (20). By simple inspection of these matrices one observes that no coupling exists between the two information channels except for the off-diagonal term q_{36} in Q. If this term is ignored and the matrices are put into the filter equations, it becomes apparent that the "optimal" filter, whose dimension is 6, consists of two noncoupled filters each of dimension 3. By treating these filters separately the computation and memory requirements are significantly reduced with respect to those of the full dimension 6 filter. Let us for later use call these filters "version A" of the decoupled filter.

The word optimal is set in quotation marks above because the filter is, of course, no longer optimal when q_{36} is set to zero since some information has been destroyed. This action corresponds to telling the filter that the position errors in the X and the Y direction due to VOR error are uncorrelated, when in fact they are correlated.

In general the two filters which result from the procedure described above are different. If the velocity error models in each channel are the same the transition matrix and the output matrix will be the same for each channel, but the noise covariance matrices for the two channels remain different as can be seen from Eq. (20). These matrices retain a dependency on the true bearing to station, α. This dependency tells the filter, in effect, to expect maximum contribution from VOR error in the X channel when $\alpha = 0$ or π, and maximum in the Y channel when $\alpha = \pi/2$ or $3\pi/2$. Upon examination of Fig. 6 it is apparent that this is the case.

For an arbitrary aircraft trajectory in the plane α will be a continually changing quantity. Consequently, the forcing noise covariances for each channel of the version A decoupled filter must be updated at each sample point. Although the updating is straightforward, it can be avoided altogether if the covariance matrices are replaced by their expected or average values. If α is uniformly distributed over the range $[0, 2\pi]$ the X channel and the Y channel covariance matrices have the same expected value. This is demonstrated by referring to Eq. (20) and using

$$E(\sin^2\alpha) = E(\cos^2\alpha) = \tfrac{1}{2}$$

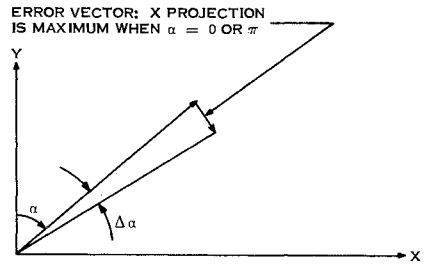

Fig. 6 VOR error projection.

Consequently if each covariance matrix is replaced by its expected values the X and Y channel filters become identical. Let us label this configuration version B of the decoupled filter.

Filter B, because it does not need to update noise covariance matrices and since it requires only one filter gain matrix (to be used in both channels) per time step, can be realized with roughly half the machine operations required by filter A. Moreover its demand for memory should be somewhat less than that of A.

The next section of the paper makes specific performance comparisons between the optimum filter and the three suboptimal filters described above. From these data the performance loss attributable to the mechanization simplifications can be judged.

Performance Comparisons

The preceding sections of this paper have been devoted to developing the theory and the techniques of both optimal and suboptimal velocity-aiding for VOR/DME systems. This section provides specific performance comparisons between the optimal and the various suboptimal filters. Data is presented for both an inertial system and an Air Data System acting as the velocity aid. The comparison is in terms of rms radial error as defined in a previous section. The error descriptions used to generate the data presented are listed in Table 2 below. All of the analyses were done with a five second sample interval for the filter since the rms estimation errors are reduced negligibly for sampling rates higher than this.

Table 2 Error parameter descriptions

Error Source	RMS Value	Correlation Time
VOR error	1.15°	10 sec
DME error	0.2 naut miles	300 sec
Air data error—X-component	40 knots	600 sec
Air data error—Y-component	40 knots	600 sec
Inertial velocity error—X-component	4 knots	600 sec
Inertial velocity error—Y-component	4 knots	600 sec

In order to have a uniform basis for comparing the performance of the various filter configurations, two basic aircraft tracks were used. Each is defined by a constant bearing-to-station; each begins 10 miles from the station and proceeds outward to 160 miles. One course bearing is 0° ($\alpha = 0$) whereas the other is 45° ($\alpha = 45$). At the start of each flight each of the two velocity integrators is assumed to have a 2 mile rms initial condition error.

Optimum Performance

Figure 7 is a performance comparison between the unaugmented VOR/DME system and two optimally-aided VOR/DME systems, one using Air Data and the other using inertial velocity. The graph shows the Air Data-aided and the inertially-aided system are better than unaided VOR/DME by factors of at least 2.5 and 5, respectively. Inertial aiding is more effective than Air Data aiding because inertial velocity is much better quality than Air Data.

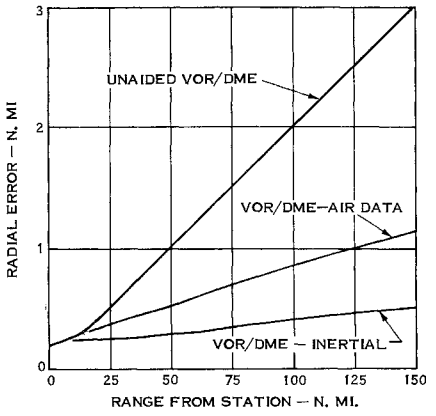

Fig. 7 Performance comparison-optimal systems vs unaided VOR/DME.

Suboptimal Performance

Performance with DME error unmodeled

Figure 8 compares the performance of the optimal, inertially-aided system with that of the same system when the DME error is not modeled in the filter. It is clear that performance loss due to not modeling DME error is not significant except perhaps very near the station.

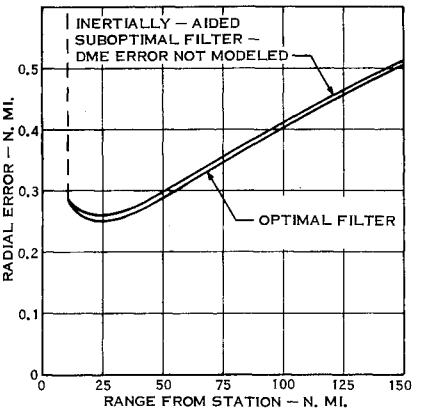

Fig. 8 Performance with DME error unmodeled.

Performance of version B mechanization

Version B of the suboptimal mechanization as described earlier consists of identical filters applied to each of the information channels. The actual covariances of the white noise vectors driving the two channels are replaced with their average value

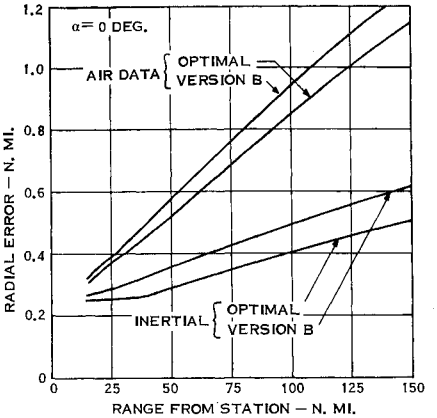

Fig. 9 Optimal filter vs version B—both air data and inertial aiding.

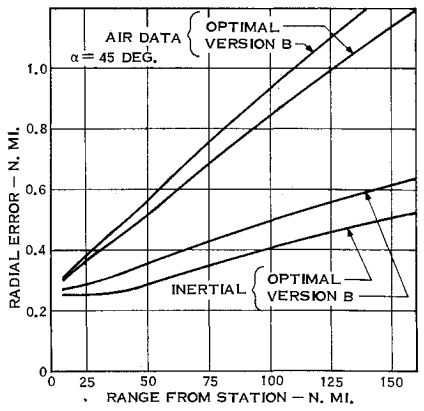

Fig. 10 Optimal filter vs version B—both air data and inertial aiding.

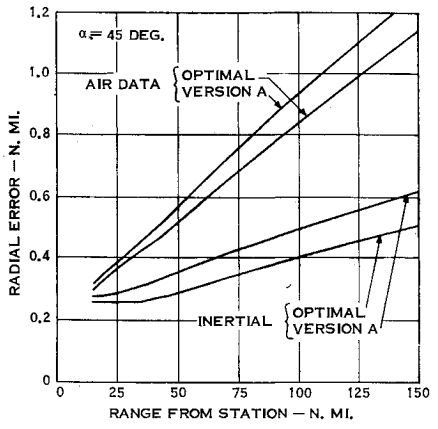

Fig. 11 Optimal filter vs version A—both air data and inertial aiding.

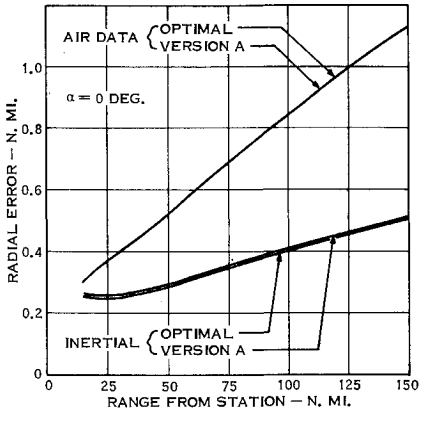

Fig. 12 Optimal filter vs version A—both air data and inertial aiding.

(averaged over α). It is this simplification which makes the two filters identical.

The performance of this mechanization is compared to the optimal in Figs. 9 and 10 for the $\alpha = 45°$ and the $\alpha = 0°$ courses. Plots are given for both inertial and Air Data aiding. The salient characteristics of this data are: 1) the performance degradation with respect to optimal is nearly the same along both courses. 2) with inertial aiding the degradation is roughly 20% while with Air data it is only 10%.

Performance of version A mechanization

The version A suboptimal mechanization as described previously consists of two decoupled filters each of which has its own bearing-dependent covariance which tells it what error magnitudes to expect. Because of this tuning effect one would expect version A performance to be somewhat better than version B.

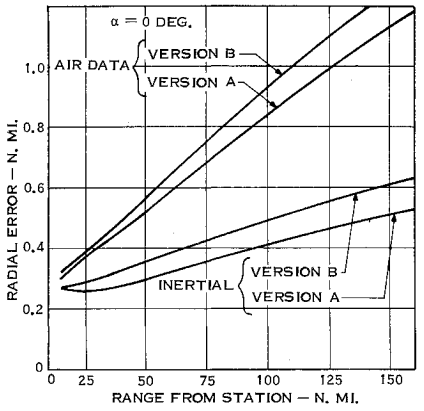

Fig. 13 Comparison between version A and version B filters—both air data and inertial aiding.

Figures 11 and 12 compare version A performance to optimal. Figure 11 is plotted for the $\alpha = 45°$ course while Fig. 12 gives plots for the course $\alpha = 0°$. The significant conclusions from the data are: 1) for $\alpha = 0$ this mechanization is essentially as good as the optimal one; and 2) for $\alpha = 45$ the degradation is about 20% for intertial aiding and 10% for Air Data aiding.

The first item above is a consequence of the fact that the principal assumption used to arrive at the decoupled mechanization is satisfied when $\alpha = 0$. That the VOR error contribution in the two channels is uncorrelated is clearly true in this case as can be seen by examining either Fig. 6 or Eq. (17).

Comparison of version A and version B

Comparisons between the performance of the A and the B mechanizations are quite interesting. By examining Figs. 10 and 11 we can see that A and B perform identically for $\alpha = 45°$. The reason is that the actual covariances, those used in A, equal the average covariances, those used in B. Thus in this case the A and B versions are identical. The same conclusion holds when $\alpha = 3\pi/4, 5\pi/4, 7\pi/4$.

On the other hand, examination of Figs. 9 and 12 reveals that A and B perform quite differently for $\alpha = 0$. In this case A is operating with correct covariances while B, using average values, is not. The pertinent data from Figs. 9 and 12 are presented in Fig. 13. This figure shows that A is superior to B by 10% when the velocity source is Air Data and by 20% when the velocity source is inertial. The same statement can be made about other courses where the bearing is a multiple of $\pi/2$.

The conclusions one can draw from these relative performance curves are: 1) deletion of the DME error from the filter model incurs essentially no performance penalty; 2) suboptimal mechanizations A and B suffer a performance penalty not exceeding 10% when Air Data is the velocity source and 20% when inertial velocity is used; and 3) version A is definitely somewhat superior to version B because of its more precise representation of forcing function covariances.

Summary and Conclusions

This paper has shown how VOR/DME measurements can be complemented with velocity data to produce significantly improved positional accuracy. An heuristic discussion on the nature of the two data sources and how they should be combined was given. Error models for both the VOR/DME system and the velocity source were developed, and the optimal system mechanization based on these models was formulated. In order to reduce mechanization complexity three separate suboptimal schemes

were developed. Finally optimal performance was compared to unaugmented VOR/DME performance, and the performance of the various suboptimal mechanizations was compared to the optimal.

The major conclusions of the paper are: 1) optimal velocity-aiding for VOR/DME produces a system whose positional accuracy is significantly better than that of unaided VOR/DME —better by a factor of 2.5 when Air Data is used and by a factor of 5 when inertial velocity is used. 2) The DME error model can be omitted from the mechanization with essentially no performance penalty. 3) The coupling between channels produced by VOR error can be omitted with moderate performance loss. The dimension 6 optimal mechanization is thereby reduced to two dimension 3 filters. 4) The performance degradation of the decoupled mechanization does not exceed 20% when inertial velocity is the aid and 10% when Air Data is employed.

References

[1] Anderson, S. R., "VHF Omnirange Accuracy Improvements," *IEEE Transactions on Aerospace and Navigational Electronics*, Vol. ANE-12, No. 1, March 1965, pp. 26–35.

[2] Flint, R. B. and Holm, E. R., "VOR Evolutionary System Improvements in the United States," *IEEE Transactions on Aerospace and Navigational Electronics*, Vol. ANE-12, No. 1, March 1965, pp. 46–57.

[3] Pitman, G. R., ed., *Inertial Guidance*, Wiley, New York, 1962.

[4] Kalman, R. E., "A New Approach to Linear Filtering and Prediction Problems," *ASME Journal of Basic Engineering*, Vol. 82, No. 1, March 1960, pp. 35–45.

[5] Laning, J. H and Battin, R. H., *Random Processes in Automatic Control*, McGraw-Hill, New York, 1956.

JANUARY 1972 AIAA JOURNAL VOL. 10, NO. 1

Stability of Solution of Systems of Linear Differential Equations with Harmonic Coefficients

F. C. L. Fu* and S. Nemat-Nasser†
Northwestern University, Evanston, Ill.

Considered is a system of linear differential equations with harmonic coefficients which are proportional to a small parameter ε. The stability of the solution is studied for case in which the corresponding autonomous system of equations, obtained by setting $\varepsilon = 0$, is in the Jordan canonical form with two equal nonzero characteristic values. A perturbation method is used, and it is shown that certain additional instability regions exist, whose description involves fractional powers of ε. In addition to several new results, some of the previous findings are deduced as special cases.

1. Introduction

THE stability analysis for systems of linear differential equations with periodic coefficients, has received considerable attention in the literature, since such systems arise naturally in the study of many physical problems. Noteworthy investigations in this area are by Cesari,[1] Mettler,[2,3] Hale,[4–6] Gambill,[7,8] Cesari and Bailey,[9] Valeev, [10–12] Hsu, [13,14] and Lion[15]; for further references, see Cesari.[1] These investigations are, however, restricted to cases where the so-called stiffness matrix of the corresponding autonomous system of equations [that is, the system obtained by setting $\varepsilon = 0$ in Eq. (1)], has a diagonal form with nonzero, distinct, positive elements. Thus, to the knowledge of the authors, no results exist in the case of a system of the form

$$\ddot{x}_\alpha + \varepsilon \sum_{\beta=1}^{n} C_{\alpha\beta}\dot{x}_\beta + \sum_{\beta=1}^{n} (A_{\alpha\beta} + \varepsilon P_{\alpha\beta}\cos\theta t)x_\beta = 0 \qquad \alpha = 1,2,\ldots,n \tag{1}$$

where the matrices $\mathbf{C} = (C_{\alpha\beta})$ and $\mathbf{P} = (P_{\alpha\beta})$ are arbitrary and possibly nonsymmetric, and the stiffness matrix $\mathbf{A} = (A_{\alpha\beta})$ has the Jordan canonical form given by

$$\mathbf{A} = \begin{bmatrix} \sigma_1^2 & 0 & 0 & . & . & \ldots & 0 \\ 0 & \sigma_2^2 & 0 & . & . & \ldots & 0 \\ \vdots & \vdots & & & & & \\ 0 & 0 & 0 & \sigma_J^2 & 0 & \ldots & 0 \\ 0 & 0 & 0 & 1 & \sigma_J^2 & \ldots & 0 \\ \vdots & \vdots & \vdots & \vdots & \vdots & & \vdots \\ 0 & 0 & 0 & 0 & 0 & \ldots & \sigma_n^2 \end{bmatrix} \tag{2}$$

in which σ_α, $\alpha = 1,2,\ldots,n$, $\alpha \neq J$, $J+1$, and σ_J are all (positive) real and distinct numbers. All the previous investigations appear to have been confined to cases in which the stiffness matrix has the following diagonal form

$$\mathbf{A} = \text{diag}(\sigma_1^2, \sigma_2^2, \ldots, \sigma_n^2) \tag{3}$$

although more general periodic coefficients than that considered in Eq. (1), have been included.

The purpose of the present paper is to study the stability of the solutions of system Eq. (1) with matrix **A** defined by Eq. (2). To this end we use a method which we presented recently.[16] Since the analysis is somewhat complicated and involves extensive algebraic manipulations, for sake of clarity we have summarized in the following section our main results. The instability boundaries defined by Eqs. (5) and (9), which involve the fractional powers of the small parameter ε, are believed to be new. Only the first and second terms in the corresponding perturbation solutions are obtained explicitly, since the additional terms can be calculated in a routine manner, albeit this would involve extensive algebraic manipulations. As is seen from the results summarized in the next section, our method yields as special cases, the results previously obtained by others for the system without damping, i.e., $C_{\alpha\beta} = 0$, and when **A** is given by Eq. (3). In the first part of the section entitled Analyses, we present the analysis corresponding to system Eq. (1) with **A** defined by Eq. (2) for both, when the damping is present, and when it is not. Here, one of our most interesting deductions is that, in the absence of damping, the unstable autonomous system can be made stable by the addition of suitable terms with harmonic coefficients of small amplitude. When damping is present, on the other hand, the system is totally unstable. On the other hand, when the matrix **A** has the diagonal form given by Eq. (3), the system Eq. (1) may or may not be stable, depending on the excitation frequency θ, and other parameters. In the last section we give two illustrative examples, in order to demonstrate that the stability conditions obtained here can be fulfilled in rather

Received March 3, 1971; revision received August 24, 1971. This research was supported by the National Science Foundation under Grant GK-27141 to Northwestern University.

* Visiting Graduate Student from the University of California at San Diego.

† Professor. Member AIAA.